Am J Transl Res 2021;13(8):8611-8631
www.ajtr.org /ISSN:1943-8141/AJTR0125361

Original Article

An integrated analysis of enhancer RNAs in glioma and a validation of their prognostic values

Han Lin[1,2*], Yong Yang[1*], Chongxian Hou[1*], Jiantao Zheng[1,3], Guangzhao Lv[1,2], Rui Mao[1,3], Peihong Xu[1,2], Shanwei Chen[1,2], Yujun Zhou[1,4], Peng Wang[1], Dong Zhou[1]

[1]Department of Neurosurgery, Guangdong Provincial People's Hospital, Guangdong Academy of Medical Sciences, Guangzhou 510080, Guangdong Province, P. R. China; [2]Shantou University Medical College, Shantou 515041, Guangdong Province, P. R. China; [3]School of Medicine, South China University of Technology, Guangzhou 510006, Guangdong Province, P. R. China; [4]Southern Medical University, Guangzhou 510515, Guangdong Province, P. R. China. [*]Equal contributors.

Received November 1, 2020; Accepted June 18, 2021; Epub August 15, 2021; Published August 30, 2021

Abstract: Glioma, a highly aggressive neuroepithelial malignant brain tumor, is associated with high disability and recurrence rates. Enhancer RNA (eRNA) plays a significant role in tumor proliferation and metastasis; however, their functions in gliomas need further evaluation. We used the computational pipeline, PreSTIGE, to predict tissue-specific enhancer-derived RNAs and the underlying regulatory genes. Using data retrieved from the TCGA and CGGA databases, a LASSO regression analysis and multiCox proportional hazards regression analyses were performed to determine the hub eRNAs associated with glioma prognosis. Quantitative reverse transcription PCR was performed on the glioma samples to evaluate the expression characteristics of the identified hub eRNAs. To construct a risk signature, we selected three eRNAs, including CRNDE, MRPS31P5, and LINC00844, for their significant prognostic values. The predictive value of the risk signature was validated using the CGGA and Rembrandt cohorts. Apart from the risk signature, the nomogram performed well at predicting OS in glioma patients. An eRNA-target gene regulatory network was established, which we evaluated using a target gene enrichment analysis. Pathway and gene ontology (GO) analyses demonstrated that the risk signature is associated with mRNA processing and spliceosome in glioma. Furthermore, we found that hub eRNAs potentially regulate the expressions of numerous splicing factors, such as MOV10 and SEC31B, and are correlated with prognosis-associated alteration splicing (AS). In conclusion, we established a risk signature that comprises three eRNAs, which can accurately be utilized as targets to predict prognosis in glioma patients.

Keywords: Enhancer RNA, glioma, prognosis, alternative splicing, splicing factor

Introduction

Glioma, one of the most common malignant brain tumors, is associated with poor prognosis. Due to glioma's high invasiveness and drug resistance, glioma patients have high disability and recurrence rates. Based on their degree of malignancy, gliomas are classified into 4 grades (i.e., WHO grades I, II, III, and IV). Among them, glioblastoma multiforme (GBM) belongs to grade IV [1]. The therapeutic options for glioma include surgery, postoperative radiotherapy, and chemotherapy. However, nearly all GBM patients who accept the first-line treatment exhibit disease progression after a median PFS of 7 to 10 months. Unfortunately, there are no efficient rescue treatments that can reliably improve glioma patients' survival outcomes [2]. Therefore, the evaluation of glioma tumorigenesis and its biomarkers will inform the development of effective therapeutic strategies.

Initially described as short DNA fragments, enhancer binds with transcription factors (TF) and transcription co-activators of histone acetylation positively drive target gene expression. Advances in high-throughput sequencing methods have enabled studies on the molecular features of the enhancers. For instance, a transcript of the enhancer exists. eRNA transcription is bidirectional and is correlated with chromatin modifications or the cofactors (H3K27ac, p300, H3K4me1, etc.). eRNAs facilitate the establishment of the promoter-enhancer com-

plex by interacting with TF and RNA polymerase II [3]. Enhancer RNAs regulate transcription in various human cells and tissues. Mutations in the eRNA elements of ACTRT1 alter enhancer activity and target gene expression, resulting in the dysregulation of Hedgehog signaling and tumor proliferation [4]. Furthermore, elevated expressions of AP001056.1 are correlated with poor prognoses in head and neck tumor patients [5]. A pan-cancer analysis revealed that an enhancer (chr9: 5580709-5581016, hereafter called enhancer-9, located ~140 kb from PD-L1), shows strong co-expression associations with the PD-L1 mRNA levels in multiple cancer types, implying that this enhancer can modulate the PD-L1 activation [6]. However, studies on the role of eRNAs in gliomas are not comprehensive.

In this study, three prognosis-associated eRNAs were identified and used to construct a risk signature that can predict survival outcomes for glioma patients. Additionally, we established enhancer RNA regulatory networks composed of hub eRNAs and target genes and explored the pathways and biological functions associated with the risk signature. Notably, the risk signature showed the potential to be utilized as a biomarker for glioma diagnosis and therapy.

Methods

Data mining

The RNA-seq data for putative eRNAs and their clinicopathological data were downloaded from the GBM and LGG datasets in *The Cancer Genome Atlas* database (TCGA, https://portal.gdc.cancer.gov/). Data for the 693 cohorts and the 325 cohorts in the Chinese Glioma Genome Atlas (CGGA, http://www.cgga.org.cn/) and the Rembrandt cohort (GSE108476, www.ncbi.nlm.nih.gov/geo) were used to validate the results. Subsequently, we processed RNA-seq data through normalization and log2 transformation.

Identifying candidate eRNAs in glioma

lncRNAs transcripted from active tissue-specific enhancers and their potential target genes were explored using *Predicting Specific Tissue Interactions of Genes and Enhancers* (PreSTIGE, https://galaxyproject.org/use/prestige/) [7]. Then, BioMart (https://www.ensembl.org) was used to convert the Ensembl transcript ID to a gene symbol for further analysis. Spearman correlation analyses were performed to evaluate the correlations between the eRNA levels and the predicted target genes. Putative eRNAs that were correlated with the levels of their target genes ($|R|>0.4$, $P<0.001$) and overall survival (OS, $P<0.05$) were considered candidate eRNAs in glioma. Additionally, the CGGA database was used to validate the prognostic value of candidate eRNAs.

Constructing and validating the eRNA prognostic model

The least absolute shrinkage and selection operator (LASSO) model is a type of regression method for multiple linear problems, and it can be used for parameter estimation and variable selection. In this study, we determined the candidate eRNAs suitable for the prediction model (iteration = 1000) using the lasso model and subjected them to multivariate Cox proportional hazards regression analyses. Through the mentioned analyses, hub eRNAs were selected from the candidate eRNAs to construct a risk model where each sample's risk score was calculated according to the following formula:

risk Score = Σ_i^n expression level of hub eRNA (i) * β (i) (β: coefficient of hub eRNA).

A log-rank test was performed to compare the differences in OS between the low- and high-risk groups. The prognostic model's performance was evaluated in terms of the area under the receiver operating characteristic curve (ROC) [8]. Patients from the CGGA and Rembrandt cohorts were used to validate the model. Using the rms R-package, a nomogram (a statistical model with a user-friendly graphical interface) was established to predict the OS outcomes for the glioma patients. We used a calibration plot to assess the nomogram's capacity.

Verification of the expressions and the prognostic values of the hub eRNAs

The associations between the expressions of the hub eRNAs and the clinicopathological features were evaluated using the TCGA cohort. Furthermore, quantitative reverse transcription PCR (qRT-PCR) was performed to measure the

Table 1. The primer of hub eRNAs

Hub eRNA	Forward	Reverse
CRNDE	5'-CATGGAAAAATCAAAGTGCTCG-3'	5'-CCTTCTTCTGCGTGACAACTG-3'
LINC00844	5'-CAGAGACATAGACATGGATCTGGG-3'	5'-GAGGAAGTTTAAGTTTTGCTTAGCC-3'
MRPS31P5	5'-CGAAGGTATTACCTGCTGGGT-3'	5'-GGCAAGTCATCTTATCTTTCTGGG-3'
GAPDH	5'-GAACGGGAAGCTCACTGG-3'	5'-GCCTGCTTCACCACCTTCT-3'

expression levels of the hub eRNAs in 40 glioma samples from Guangdong Provincial People's Hospital. Then we verified the prognostic value of the hub eRNAs in the gliomas based on the corresponding clinicopathological data of the glioma samples (Supplementary Table 1).

Constructing the eRNA-target gene regulatory network and the functional analysis

We performed Spearmen correlation analyses to assess the correlation between the hub eRNAs and their target genes based on the TCGA database. Next, the target genes (Spearmen's rank correlation analysis $|r|>0.4$, $P<0.001$) were selected to construct the eRNA-target gene regulatory network and to perform further functional analyses. Gene ontology (GO) and *Kyoto Encyclopedia of Genes and Genomes* (KEGG) analyses were performed on the detected target genes to establish their functions ($P<0.05$).

Downloading and processing alterative splicing (AS) data

From the TCGASpliceSeq database (https://bioinformatics.mdanderson.org/TCGASpliceSeq/), as profiles were downloaded to assess mRNA splicing patterns in glioma patients. Quantifying the AS events, the Percent Spliced In (PSI) values were used to determine the seven types of alternative splicing events: Alternate Acceptor site (AA), Alternate Donor site (AD), Alternate Terminator (AT), Alternate Promoter (AP), Retained Intron (RI), Mutually Exclusive Exons (ME), and Exon Skip (ES).

Using UpSet-R (version 1.3.3), we generated distinguishable visualization UpSet plots to quantitatively analyze the intersections between the AS events and the risk signature in glioma. The associations between the splicing factors and the alternative splicing events were further analyzed under the Pearson correlation coefficient threshold $>|0.6|$, $P<0.001$.

Quantitative reverse transcription PCR (qRT-PCR)

A total of 40 glioma samples were used for the qRT-PCR verification of the expression of hub eRNAs. Total RNAs from the samples were extracted using the trizol reagent (AG21102, Accurate Biotechnology, Hunan, China). cDNA was synthesized with the RT Premix for qPCR (AG11706, Accurate Biotechnology, Hunan, China) in the Reverse Transcription System (Biometra Advanced). The RT-PCR conditions were: 37°C for 15 min, 85°C for 5 s, and 4°C hold. qRT-PCR was performed on the cDNA using SYBR GREEN kits (Accurate Biotechnology, Hunan, China) in the BIO-RAD CFX connect Real-Time PCR System. The mixes were pre-denaturized at 95°C for 10 min, followed by 40 cycles of denaturation at 95°C for 5 s, 60°C for 30 s and 72°C for 30 s. The 2-ΔCt method was used to calculate the relative expression levels of the hub eRNAs, which were presented as the means with SD. The primers used are shown in **Table 1**.

Statistical analysis

The correlation plots of the hub eRNAs and the corresponding splicing factors were visualized in Cytoscape (version 3.6.0). Wilcoxon tests were used to compare the differences in the expression levels of the three hub eRNAs and the risk signatures between the groups. Overall survival (OS) was presented as a Kaplan-Meier curve, according to the median value of the hub eRNAs' expressions or risk scores. The statistical data were analyzed using R/Bioconductor (version 3.6.1). Moreover, $P<0.05$ was considered statistically significant.

Results

Prognosis-related eRNAs

Figure 1 is a schematic presentation of the study design. We identified a total of 2,880 ENCODE (*Encyclopedia of DNA Elements* data-

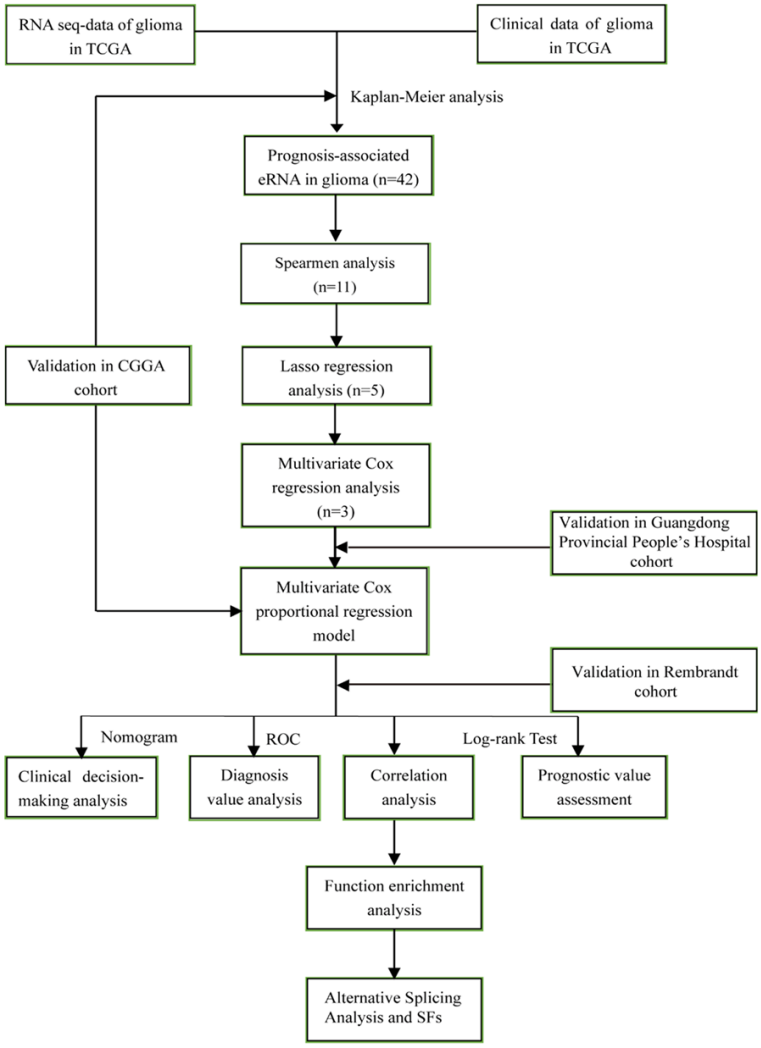

Figure 1. Schematic presentation for the analysis of eRNAs in glioma.

base, https://www.encodeproject.org/) annotated lncRNA transcripts, which were transcripted from active tissue-specific enhancers and from the 2,304 predicted target genes based on the PreSTIGE algorithm. To facilitate the data processing and the exploration in the TCGA and CGGA databases, Ensembl BioMart (http://asia.ensembl.org/info/data/biomart/index.html) was used to convert the transcript ID to a gene ID. Next, the 1,406 putative eRNA transcripts were mapped to their corresponding 1,406 genes. Subsequently, using the RNA-sequencing data from the 692 glioma patients in the TCGA database and the 929 patients in the CGGA database, 42 of the 1,406 putative eRNA genes associated with glioma patient survival were identified ($P<0.05$). Our Spearman's rank correlation analyses revealed that the mRNA expression levels for the 11 eRNAs were correlated with the mRNA expression levels of their targeted genes (**Table 2** and **Figure 2**). To establish the prognostic significance of the 11 eRNAs, lasso regression analyses were performed, whereby we obtained five prognostic-associated eRNAs (**Figure 3A** and **3B**). Furthermore, the five prognostic-associated eRNAs were subjected to multiple stepwise Cox regression analyses, from which three hub eRNAs were identified (**Figure 3C**).

Verification of the expression levels and the prognostic values of hub eRNAs

The expression levels of the three hub eRNAs were correlated with the WHO grades and the glioma IDH statuses. With an increase in the glioma grade, the CRNDE expression increased (**Figure 4A** and **4B**) and the LINC00844 and MRPS31P5 expressions decreased (**Figure 4E**, **4F**, **4I** and **4J**). In addition, the CRNDE expression was upregulated (**Figure 4C** and **4D**), but the LINC00844 and MRPS31P5 expressions were suppressed in the IDH wildtype gliomas, compared to the IDH mutant samples (**Figure 4G**, **4H**, **4K**, and **4L**). In addition to the glioma sample expression and clinical data from the Guangdong Provincial People's Hospital, we further validated the prognostic value of the three hub eRNAs in glioma (**Figure 4M-O**).

Construction and analysis of the prognostic signature

A prognostic signature was established based on the hub eRNAs. The risk score for each patient was calculated according to the formula:

Risk score = (-0.10905 * ExpLINC00844) + (0.24722 * ExpCRNDE) + (-0.34714 * ExpMRPS31P5).

Table 2. The eRNAs associated with glioma patients' survival and their predicted targeted genes

eRNA	*P*-value of KM (TCGA)	*P*-value of KM (CGGA)	Target	Cor (TCGA)	*P*-value of Cor
LINC01088	0.00129281	4.70E-12	NAA11	0.88876	5.50E-238
HCP5	2.01E-05	1.84E-09	MICB	0.553877	0
TP53TG1	0.014471187	0.00233817	CROT	0.512476	0
SSPO	0.002109041	0.00027333	ZNF862	0.437471	0
LINC00689	6.51E-07	5.91E-11	VIPR2	0.880249	1.60E-227
LINC00844	3.71E-05	0	PHYHIPL	0.473788	0
LINC00601	1.53E-06	0	ADAM12	0.488035	4.73E-43
MRPS31P5	0.030106381	1.16E-05	ATP7B	0.547907	6.18E-56
			NEK3	0.44947	5.22E-36
CRNDE	0	0	IRX5	0.843398	6.02E-190
LINC00665	8.22E-06	0	ZFP14	0.590735	6.94E-67
			ZFP82	0.582864	0
			ZNF146	0.633844	0
			ZNF260	0.707048	0
DGCR5	0.028838174	0	PRODH	0.401513	0

P<0.05, a significant difference.

In the TCGA cohort, the low-risk group of patients exhibited better prognostic outcomes than the patients in the high-risk group (**Figure 5A**). Our time-dependent ROC analysis suggested that the model has a satisfactory diagnostic performance for glioma (**Figure 5B**). Moreover, our scatter plots and heatmap showed the correlations between the risk scores of the signature and the survival statuses of the patients in the low-risk and high-risk subgroups (**Figure 5C** and **5D**). Furthermore, the results from the CGGA and Rembrandt cohorts were used to validate the performance of the prognostic score model (**Figure 6**).

The risk signature and the clinicopathological features in glioma

The clinicopathological features (glioma age, grade, the 1p19q codel status, and the IDH status) play significant roles in the glioma prognosis. The risk signatures of glioma patients <60 years were lower than those of older patients (aged ≥60) (**Figure 7A** and **7F**). With the different grades, the risk signatures of LGG (grades II and III) were lower than the risk signatures of GBM (WHO grade IV) (**Figure 7C** and **7H**). The risk signature was higher in the IDH wildtype glioma compared to the risk signature in the IDH mutant glioma (**Figure 7D** and **7I**). Also, the glioma 1p19q status correlated with glioma: the risk signatures of the 1p19q co-deletion gliomas were lower than the risk signatures of the 1p19q non-codeletion ones (**Figure 7E** and **7J**). Furthermore, the patients with high-risk scores had poorer prognostic outcomes than those with low-risk scores in both lower-grade glioma (LGG) and glioblastoma (GBM) (**Figure 7K-N**).

Establishing a hub of eRNA-related nomograms

The clinical characteristics of glioma patients are vital for their prognoses. We performed multivariate Cox regression analyses to determine their prognostic values. The three-eRNA signature was found to be a potential independent prognostic factor for glioma patients (P<0.05, **Figure 8A**). Next, a nomogram was established to evaluate the glioma patients' survival rates, which could help the neurosurgeons to create clinical plans for glioma therapy (**Figure 8B**). The calibration plots showed good conformity between the predicted and observed outcomes in both the TCGA and CGGA cohorts (**Figure 8C** and **8D**).

eRNA-target gene regulatory networks and a functional analysis of the three-eRNA risk signature

Some targeted genes (|R|>0.4) were selected for functional enrichment analyses. The biological processes that were found to be associated with glioma proliferation and invasion

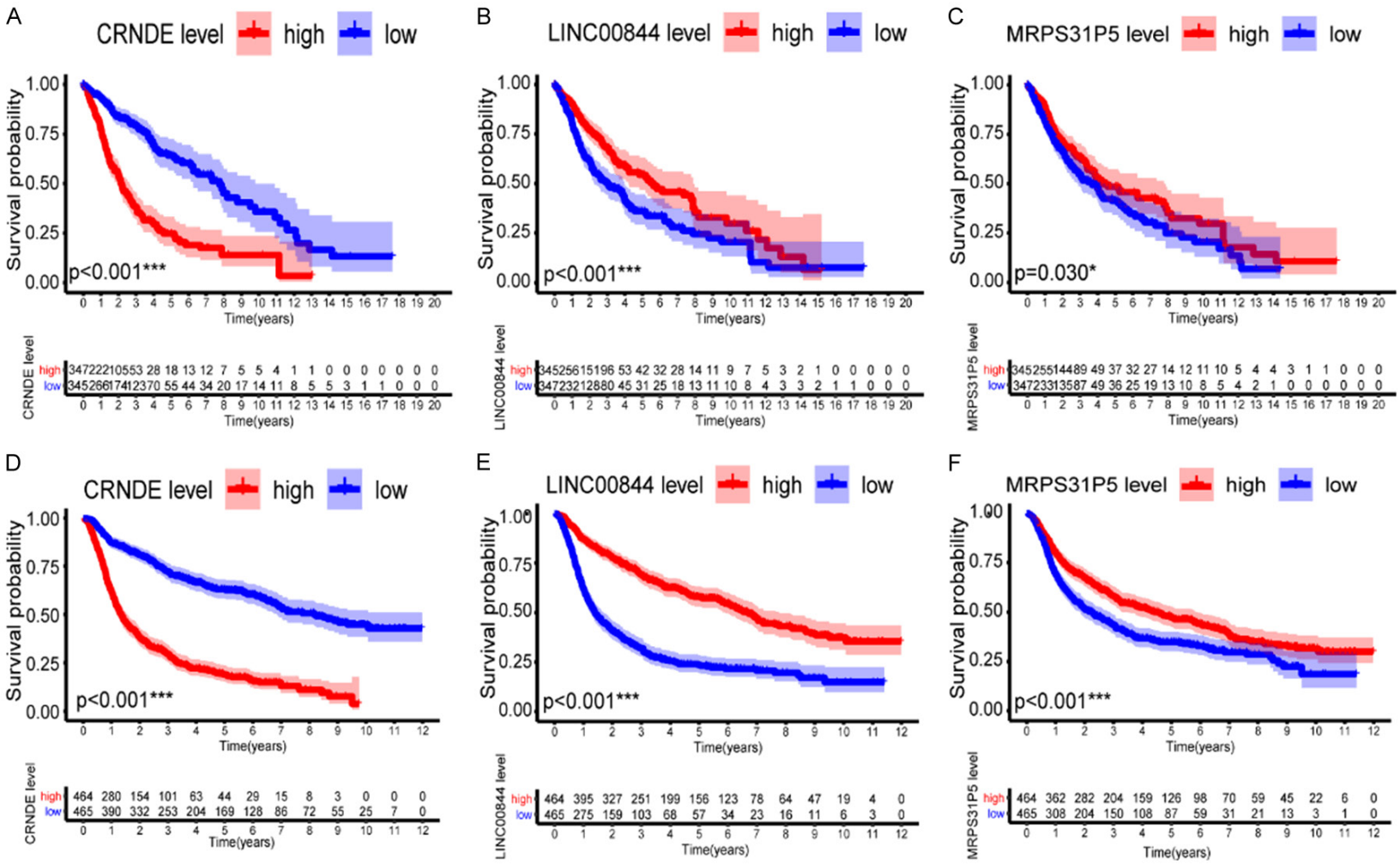
A
CRNDE level high low
Survival probability
p<0.001***
Time(years)
CRNDE level
high 347 222 105 53 28 18 13 12 7 5 5 4 1 1 0 0 0 0 0 0 0
low 345 266 174 123 70 55 44 34 20 17 14 11 8 5 5 3 1 1 0 0 0
B
LINC00844 level high low
Survival probability
p<0.001***
Time(years)
LINC00844 level
high 345 256 151 96 53 42 32 28 14 11 9 7 5 3 2 1 0 0 0 0 0
low 347 232 128 80 45 31 25 18 13 11 10 8 4 3 3 2 1 1 0 0 0
C
MRPS31P5 level high low
Survival probability
p=0.030*
Time(years)
MRPS31P5 level
high 345 255 144 89 49 37 32 27 14 12 11 10 5 4 4 3 1 1 0 0 0
low 347 233 135 87 49 36 25 19 13 10 8 5 4 2 1 0 0 0 0 0 0
D
CRNDE level high low
Survival probability
p<0.001***
Time(years)
CRNDE level
high 464 280 154 101 63 44 29 15 8 3 0 0 0
low 465 390 332 253 204 169 128 86 72 55 25 7 0
E
LINC00844 level high low
Survival probability
p<0.001***
Time(years)
LINC00844 level
high 464 395 327 251 199 156 123 78 64 47 19 4 0
low 465 275 159 103 68 57 34 23 16 11 6 3 0
F
MRPS31P5 level high low
Survival probability
p<0.001***
Time(years)
MRPS31P5 level
high 464 362 282 204 159 126 98 70 59 45 22 6 0
low 465 308 204 150 108 87 59 31 21 13 3 1 0

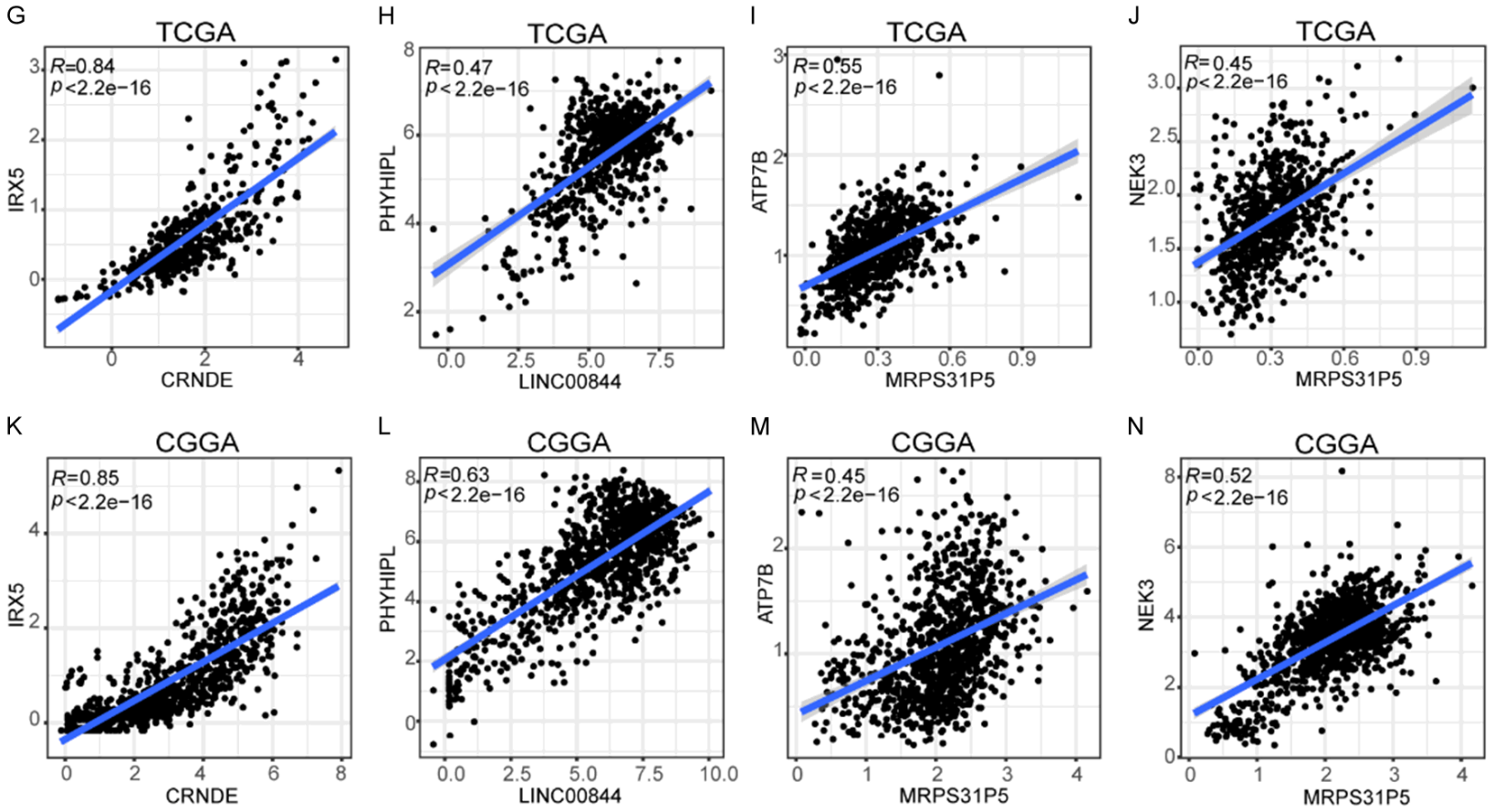

Figure 2. Prognostic values and predicted target genes for key eRNAs in glioma. A. The effect of CRNDE on glioma patients in the TCGA cohort. B. The effect of LINC00844 on glioma patients in the TCGA cohort. C. The effect of MRPS31P5 on glioma patients in the TCGA cohort. D. The effect of CRNDE on glioma patients in the CGGA cohort. E. The effect of LINC00844 on glioma patients in the CGGA cohort. F. The effect of MRPS31P5 on glioma patients in the CGGA cohort. G. A correlation analysis of CRNDE and its predicted targeted gene, IRX5, in the TCGA cohort. H. A correlation analysis of LINC00844 and its predicted targeted gene, PHYHIPL, in the TCGA cohort. I. A correlation analysis of MRPS31P5 and its predicted targeted gene, ATP7B, in the TCGA cohort. J. A correlation analysis of MRPS31P5 and its predicted targeted gene, *NEK3*, in the TCGA cohort. K. A correlation analysis of CRNDE and IRX5 in the CGGA cohort. L. A correlation analysis of LINC00844 and PHYHIPL in the CGGA cohort. M. A correlation analysis of MRPS31P5 and ATP7B in the CGGA cohort. N. A correlation analysis of MRPS31P5 and NEK3 in the CGGA cohort. IRX5: Iroquois homeobox 5; PHYHIPL: phytanoyl-CoA 2-hydroxylase interacting protein like; ATP7B: ATPase copper transporting β; NEK3: NIMA related kinase 3. *, $P<0.05$; **, $P<0.01$; ***, $P<0.001$.

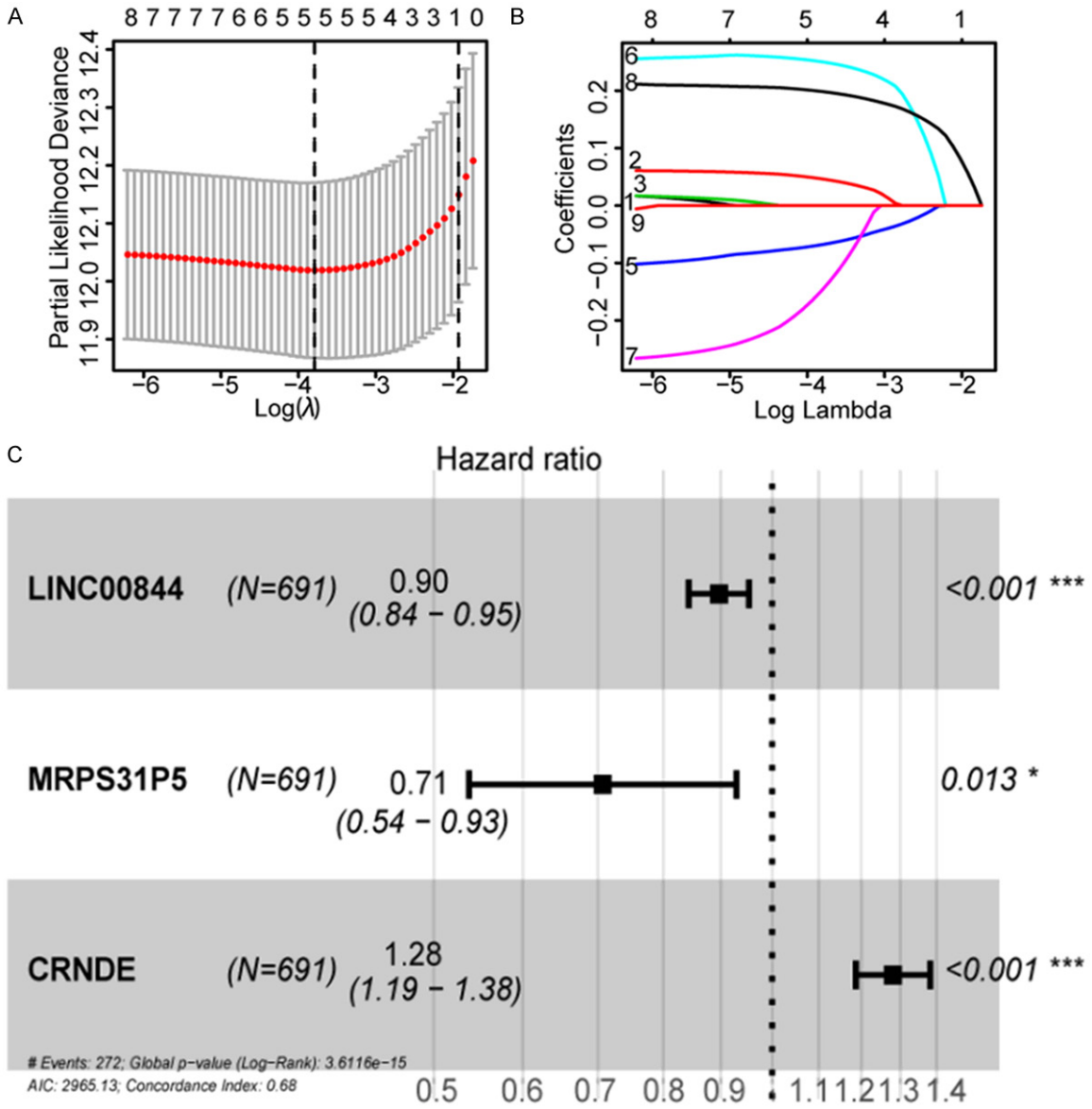

Figure 3. Identification of the hub eRNAs. A. Partial likelihood deviance of the lasso regression analysis of candidate eRNAs. B. Coefficients of the lasso regression analysis of candidate eRNAs. C. Multivariate Cox regression analyses of the candidate eRNAs to obtain hub eRNA. *, $P<0.05$; **, $P<0.01$; ***, $P<0.001$.

included histone modification, microtubule cytoskeleton organization, and mRNA processing (**Figure 9A-D**). Several KEGG pathways, including the FoxO signaling pathway, spliceosome, autophagy (animal), RNA degradation, and the AMPK signaling pathways were identified (**Figure 9E** and **9F**).

Interestingly, the GO and KEGG analyses revealed that the target gene of the risk signature was enriched in histone modification as well as in the mRNA processing and splicing, indicating that the risk signature may be associated with splicing events in glioma. From the list of eRNA-targeted genes, 78 splicing factors were detected (Supplementary Table 2), which were then incorporated in the eRNA-splicing factor regulatory network (**Figure 10A** and **10B**). Based on the alternative splicing (AS) event data from the TCGASpliceSeq database, 16,806 AS events were associated with glioma prognoses (**Figure 10C** and **10D**). Among the 78 splicing factors, the mRNA MOV10 (Mov10 RISC Complex RNA Helicase) and SEC31B

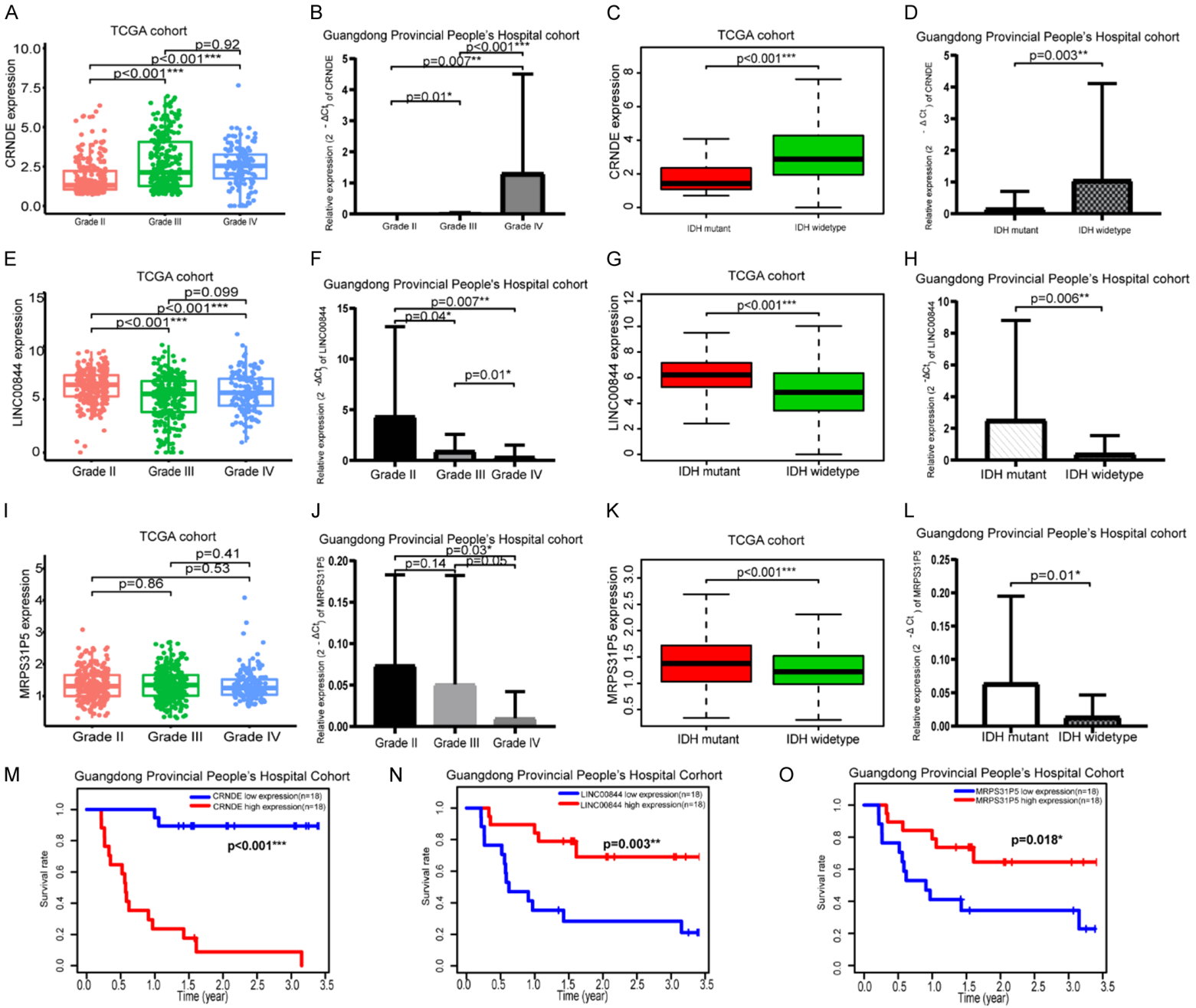
A
TCGA cohort
CRNDE expression
p=0.92
p<0.001***
p<0.001***
Grade II
Grade III
Grade IV
B
Guangdong Provincial People's Hospital cohort
Relative expression (2 - ΔCt) of CRNDE
p<0.001***
p=0.007**
p=0.01*
C
TCGA cohort
CRNDE expression
p<0.001***
IDH mutant
IDH widetype
D
Guangdong Provincial People's Hospital cohort
p=0.003**
E
TCGA cohort
LINC00844 expression
p=0.099
p<0.001***
p<0.001***
F
Guangdong Provincial People's Hospital cohort
Relative expression (2 -ΔCt) of LINC00844
p=0.007**
p=0.04*
p=0.01*
G
TCGA cohort
LINC00844 expression
p<0.001***
H
Guangdong Provincial People's Hospital cohort
p=0.006**
I
TCGA cohort
MRPS31P5 expression
p=0.41
p=0.53
p=0.86
J
Guangdong Provincial People's Hospital cohort
Relative expression (2 - ΔCt) of MRPS31P5
p=0.03*
p=0.14
p=0.05
K
TCGA cohort
MRPS31P5 expression
p<0.001***
L
Guangdong Provincial People's Hospital cohort
p=0.01*
M
Guangdong Provincial People's Hospital Cohort
CRNDE low expression(n=18)
CRNDE high expression(n=18)
p<0.001***
Survival rate
Time (year)
N
Guangdong Provincial People's Hospital Corhort
LINC00844 low expression(n=18)
LINC00844 high expression(n=18)
p=0.003**
O
Guangdong Provincial People's Hospital Cohort
MRPS31P5 low expression(n=18)
MRPS31P5 high expression(n=18)
p=0.018*

Figure 4. Verification of the expressions and the prognostic values of the hub eRNAs. A. The association between the CRNDE expression and the glioma grades in the TCGA cohort. B. The association between the CRNDE expression and the glioma grades in the Guangdong Provincial People's Hospital cohort. C. The association between the CRNDE expressions and the isocitrate dehydrogenase (IDH) status of the gliomas in the TCGA cohort. D. The association between the CRNDE expressions and the isocitrate dehydrogenase (IDH) status of gliomas in the Guangdong Provincial People's Hospital cohort. E. The association between the LINC00844 expressions and the glioma grades in the TCGA cohort. F. The association between the LINC00844 expressions and the glioma grades in the Guangdong Provincial People's Hospital cohort. G. The association between the LINC00844 expressions and the isocitrate dehydrogenase (IDH) status of the gliomas in the TCGA cohort. H. The association between the LINC00844 expressions and the isocitrate dehydrogenase (IDH) statuses of the gliomas in the Guangdong Provincial People's Hospital cohort. I. The association between the MRPS31P5 expressions and the glioma grades in the TCGA cohort. J. The association between the MRPS31P5 expressions and the glioma grades in the Guangdong Provincial People's Hospital cohort. K. The association between the MRPS31P5 expressions and the isocitrate dehydrogenase (IDH) statuses of the gliomas in the TCGA cohort. L. The association between the MRPS31P5 expressions and the isocitrate dehydrogenase (IDH) statuses of the gliomas in the Guangdong Provincial People's Hospital cohort. M. The effect of CRNDE on the glioma patients in the Guangdong Provincial People's Hospital cohort. N. The effect of LINC00844 on the glioma patients in the Guangdong Provincial People's Hospital cohort. O. The effect of MRPS31P5 on the glioma patients in the Guangdong Provincial People's Hospital cohort. *, $P<0.05$; **, $P<0.01$; ***, $P<0.001$.

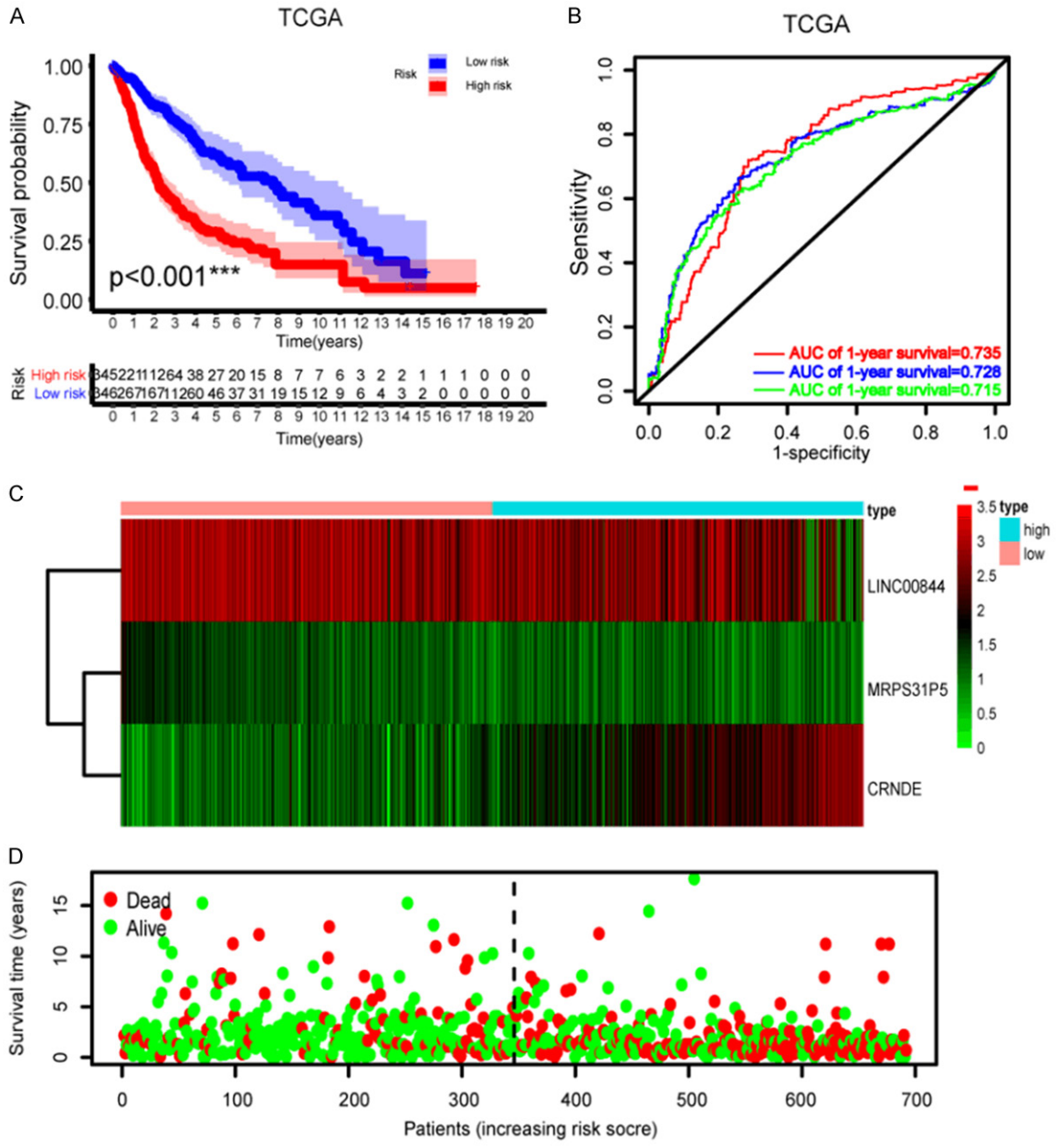

Figure 5. An analysis of the three-eRNAs signature model in the TCGA cohort. A. The effect of the risk signature on glioma prognosis in the TCGA cohort. B. An ROC analysis of the three-eRNAs signature model in the TCGA cohort. C. A heatmap showing the difference in the hub eRNA expressions between the low-risk group and the high-risk group. D. The survival statuses of the patients in the TCGA cohort. *, $P<0.05$; **, $P<0.01$; ***, $P<0.001$.

(secretory pathway component Sec31 homolog B) expression levels were correlated with the glioma prognosis in the TCGA and CGGA cohorts (**Figure 10E-H**). After evaluating the correlation between the splicing factors and the AS events, a total of 152 prognosis-associated AS events were filtered. In summary, the two key splicing factors, MOV10 and SEC31B, regulate the AS events in glioma (**Figure 10I**).

Discussion

Non-specific therapeutic options for glioma, including surgical resection, radiotherapy, and chemotherapy, have been shown to have unsatisfactory survival outcomes for glioma patients. However, currently, there is no effective targeted therapy that can improve the curative effect. lncRNAs are involved in glioma proliferation and can be regarded as potential therapeutic targets [9]. As a specific subclass of lncRNAs, eRNAs can affect the transcription of the corresponding genes in the cis-acting model [10]. With the potential to predict enhancer-gene regulatory links, eRNAs are critical for enhancer functions in the neuronal system. They are involved in the depolarization activity of neurons after stimuli [11-13]. In brain ischemia, the knockdown of some eRNAs extend the infarction region of the brain [14]. However, the functions of eRNAs in glioma have not been clearly elucidated. A convenient method, PreSTIGE provides an important avenue for researchers to predict eRNAs using RNA-seq data. After using PreSTIGE to establish long ncRNA associated with tissue-specific enhancers, we adopted the Kaplan-Meier method to evaluate the prognostic value of eRNAs in glioma. Moreover, LASSO regression and multivariate Cox regression analyses were performed to screen the hub eRNAs with prognostic significance. Then, a predictive model was established based on the expressions of the hub eRNAs. We constructed a nomogram model by integrating the risk signature and the clinicopathological factors (age, gender, grade, IDH status, and 1p19q status) to predict glioma patient survival. Finally, the functions of the risk signature were evaluated based on their highly correlated genes.

We identified CRNDE, MRPS31P5, and LINC00844 as hub eRNAs in glioma. IRX5 (Iroquois homeobox 5), the predicted target of CRNDE, has been reported to promote colorectal cancer (CRC) invasion by inhibiting the RHOA pathway in CRC cells [15]. IRX5 directly binds OPN and enhances the NF-κB luciferase activity, promoting the proliferation and migration of cancer cells in tongue squamous cell carcinoma [16]. In another study, it was observed that the elevated expression levels of CRNDE were positively correlated with IRX5 in CRC, consistent with our findings [17]. Previous studies reported that LINC00844 suppresses tumor growth and is downregulated in several tumors, including hepatocellular carcinoma and prostate tumors [18-20]. As a targeted gene of LINC00844, PHYHIPL (phytanoyl-CoA 2-hydroxylase interacting protein like) is a marker for poor prognosis in glioblastoma patients [21]. We found that the elevated expression levels of MRPS31P5 are associated with the enhanced expressions of its targeted gene ATP7B (ATPase copper transporting β) and NEK3 (NIMA Related Kinase 3). ATP7B regulates the availability of copper for oncogenic enzymes such as LOX and LOX-like proteins, conferring higher invasiveness to malignant cells [22, 23]. In breast cancer, prolactin stimulation was shown to induce the interaction between NEK3 and paxillin (a component of cytoskeleton), significantly elevating paxillin serine phosphorylation and the motility of breast cancer cells [24].

Although eRNAs have been reported to modulate targeted cis-acting genes, it has been suggested that eRNAs potentially mediate the expression of other genes [25, 26]. Several of them are important modulators of ncRNAs in tumors and play important roles in tumor proliferation, invasion, and metastasis [19, 27, 28]. We measured other co-expressed genes to evaluate the functions of these hub eRNAs. Besides the predicted target gene for eRNAs, a total of 3,374 genes were found to exhibit significant expression correlations with hub eRNAs. Apart from their correlation with the mRNA transcription process, e.g., histone modification, the gene transcripts associated with

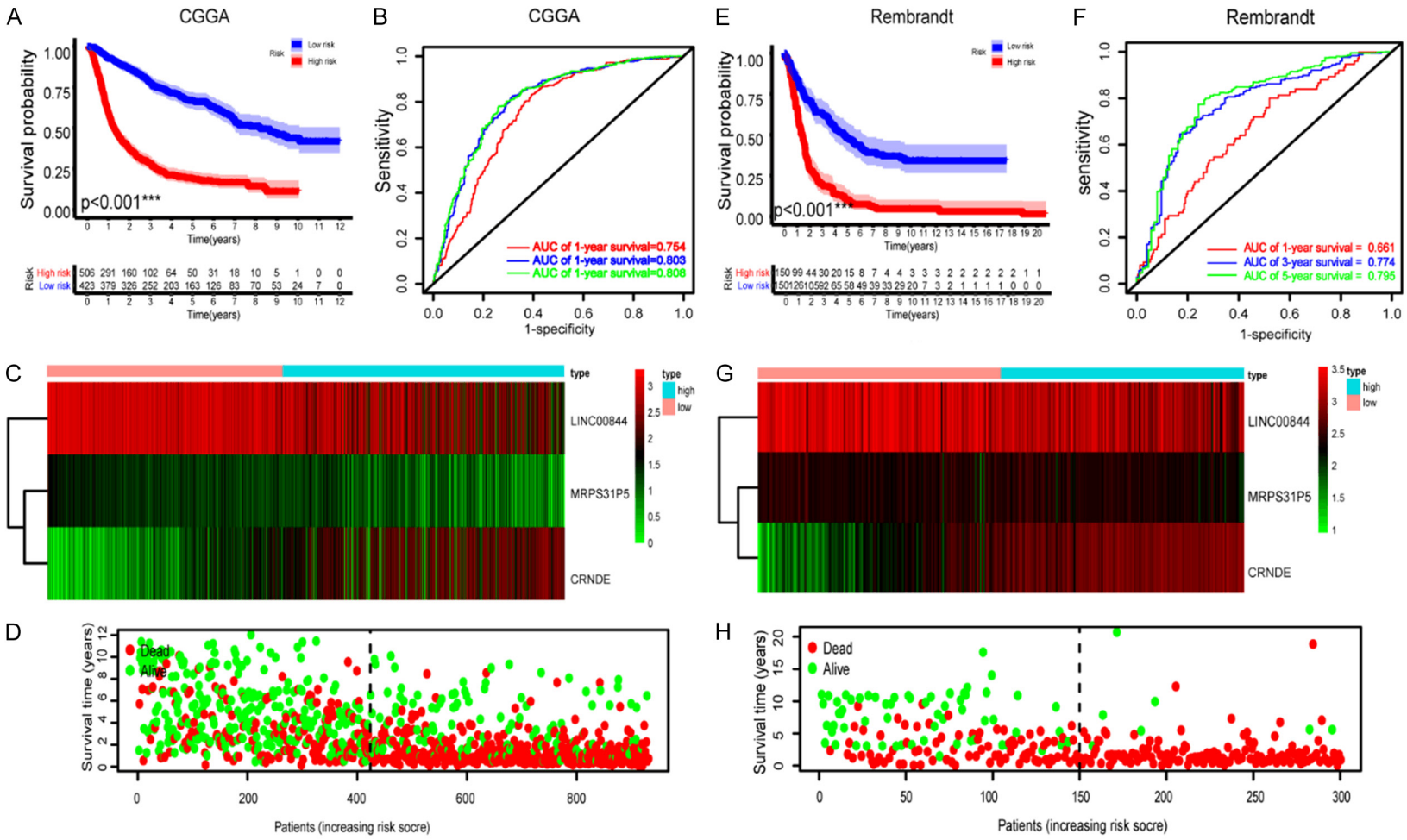

Figure 6. An analysis of the three-eRNA signature model in the CGGA and Rembrandt cohorts. A. The effects of the risk-signature on the glioma prognosis in the CGGA cohort. B. An ROC analysis of the three-eRNAs signature model in the CGGA cohort. C. A heatmap showing the difference in the hub eRNA expressions between the low-risk and high-risk groups of the CGGA cohort. D. The survival statuses of the patients in the CGGA cohort. E. The effect of the risk-signature on the glioma prognosis in the Rembrandt cohort. F. An ROC analysis of the three-eRNA signature model in the Rembrandt cohort. G. A heatmap showing the differences in the hub eRNA expressions between the low-risk and high-risk groups in the Rembrandt cohort. H. The survival statuses of the patients in the Rembrandt cohort. *, $P<0.05$; **, $P<0.01$; ***, $P<0.001$.

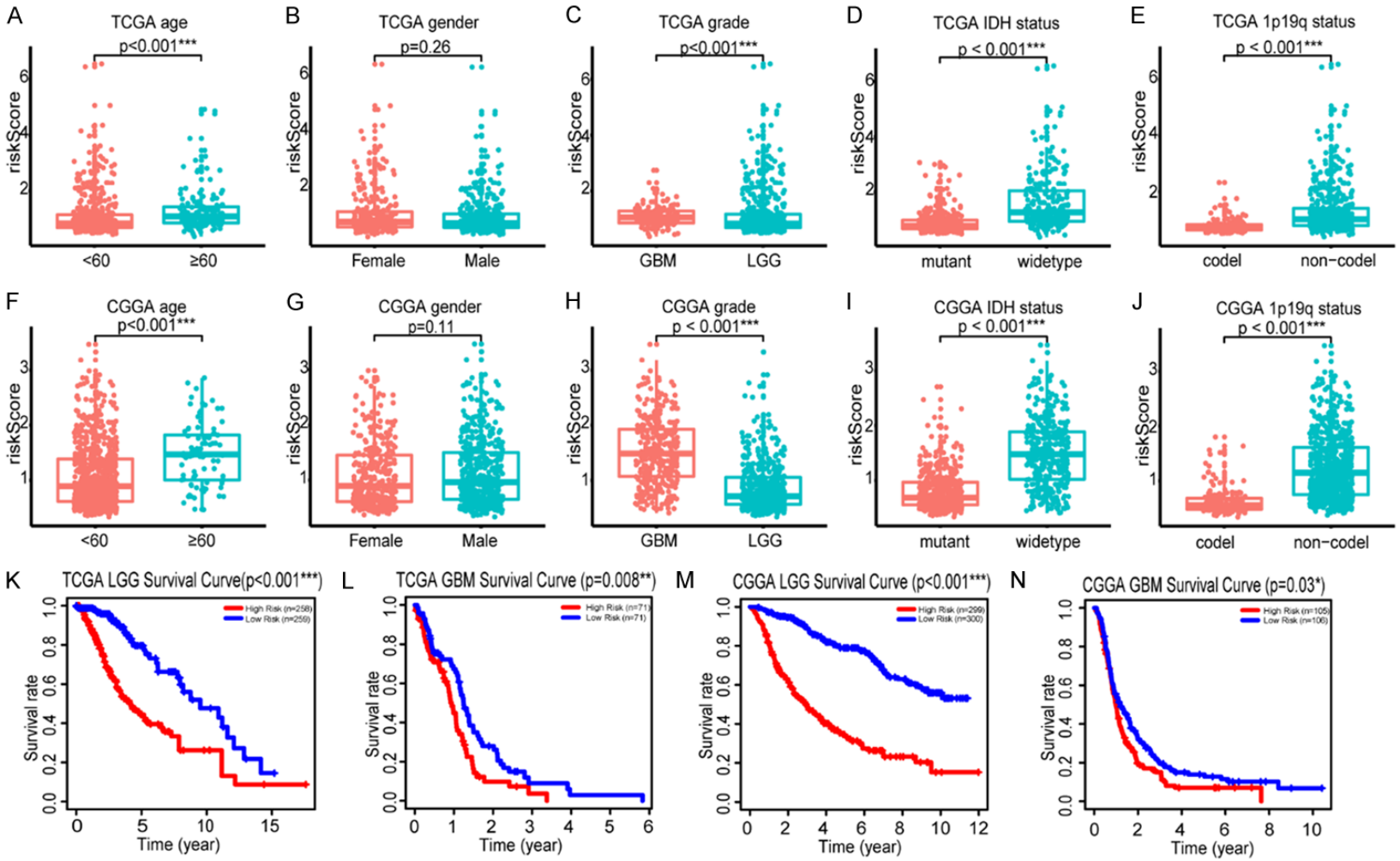

Figure 7. The prognostic values and the clinical characteristics of the three-eRNA signature in glioma. A. The association between the risk signature and the ages of the glioma patients in the TCGA cohort. B. The association between the risk signature and the genders of the glioma patients in the TCGA cohort. C. The association the between risk signature and the glioma grades in the TCGA cohort. D. The association between the risk signature and the isocitrate dehydrogenase (IDH) statuses of the gliomas in the TCGA cohort. E. The association between the risk signatures and the 1p19q statuses of the gliomas in the TCGA cohort. F. The association between the risk signatures and the ages of the glioma patients in the CGGA cohort. G. The association between the risk signature and the genders of the glioma patients in the CGGA cohort. H. The association between the risk signatures and the glioma grades in the CGGA cohort. I. The association between the risk signatures and the isocitrate dehydrogenase (IDH) statuses of the gliomas in the CGGA cohort. J. The association between the risk signature and the 1p19q statuses of the gliomas in the CGGA cohort. K. The prognostic value of the three-eRNA signatures in the LGG of the TCGA cohort. L. The prognostic value of the three-eRNA signatures in the GBM of the TCGA cohort. M. The prognostic value of the three-eRNA signatures in the LGG of the CGGA cohort. N. The prognostic value of the three-eRNA signatures in the GBM of the CGGA cohort. *, $P<0.05$; **, $P<0.01$; ***, $P<0.001$.

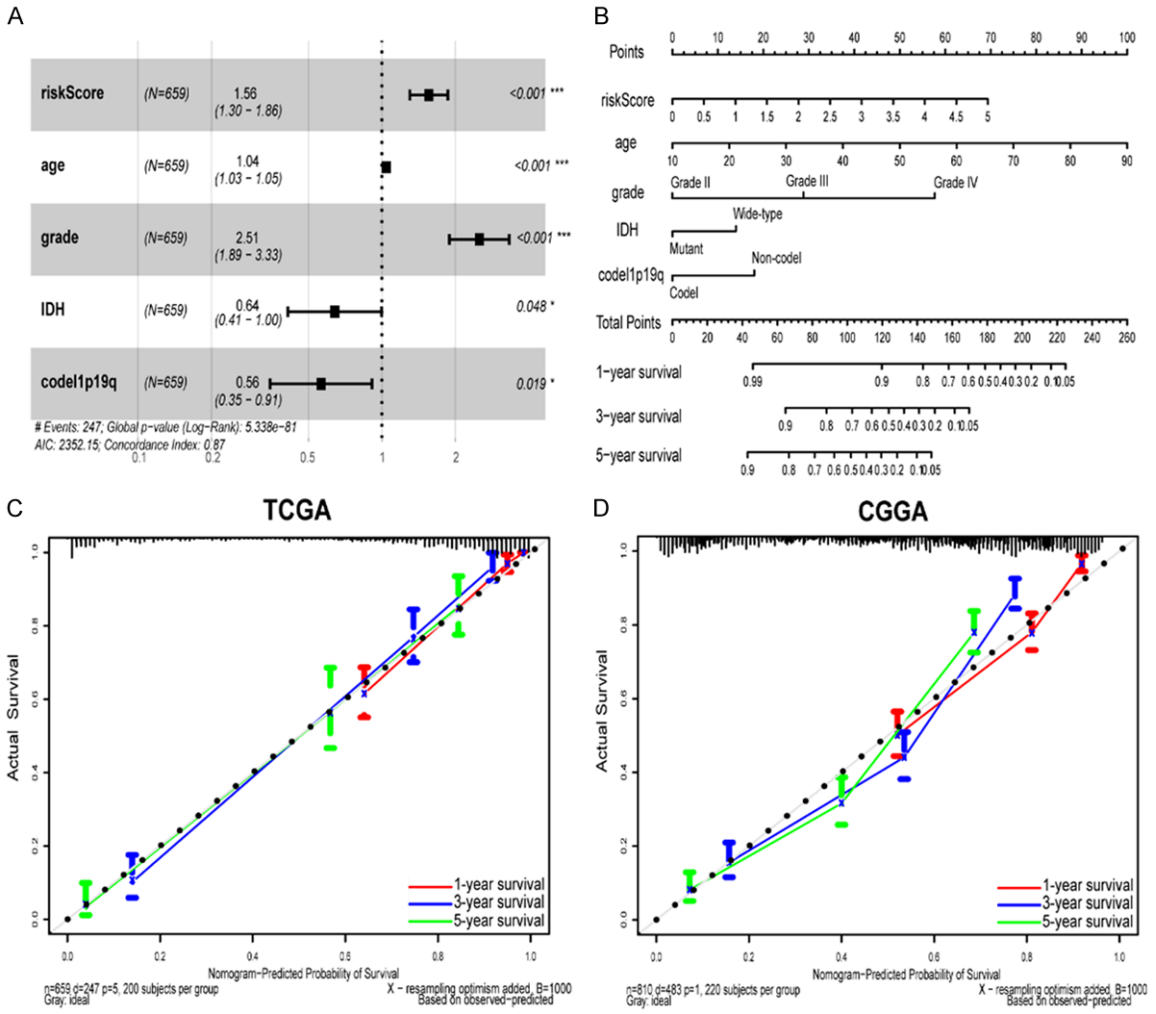

Figure 8. A Nomogram and the calibration plots of the risk signature and the clinicopathologic factors. A. A multivariate Cox regression analysis showing the risk signature as an independent prognostic factor for glioma. B. A Nomogram predicting the 1-, 3- and 5-year OS in the TCGA cohort. C. The calibration plots of the nomogram predicting OS at 1, 3, and 5 years in the TCGA cohorts. D. Calibration plots of the nomogram predicting OS at 1, 3, and 5 years in the CGGA cohorts. *, $P<0.05$; **, $P<0.01$; ***, $P<0.001$.

these hub eRNAs are mainly involved in spliceosome, nuclear speck, mRNA processing, and RNA splicing. Alternative pre-mRNA splicing plays a significant role in regulating the gene expression pathways, and it also serves as a therapeutic target in tumors [29, 30]. Small-molecule inhibitors, such as ladienolide-B or antisense-oligonucleotide have been reported to inhibit tumor growth by suppressing the splicing factor activity [31]. We found that hub eRNAs regulate the expression of 78 splicing factors and nearly 470 prognostic-associated AS events in glioma cells. Among them, MOV10 and SEC31B are regarded as the key splicing factors of the eRNA-signature, due to their prognostic value. MOV10, associated with telomerase, regulates the development of the central nervous system [32-35]. In glioma, the binding of MOV10 to cir-DICER1 promotes tumor angiogenesis through ZIC4-Hsp90β [36]. The other key splicing factor, SEC31B, has been reported to play a significant role in COP-II coat formation [37, 38]. However, experimental studies have not evaluated the correlations between these SFs and the above reported eRNAs in glioma.

Conclusion

Three eRNAs are correlated with glioma prognosis. Based on these eRNAs, a risk signature was constructed using the TCGA cohort and

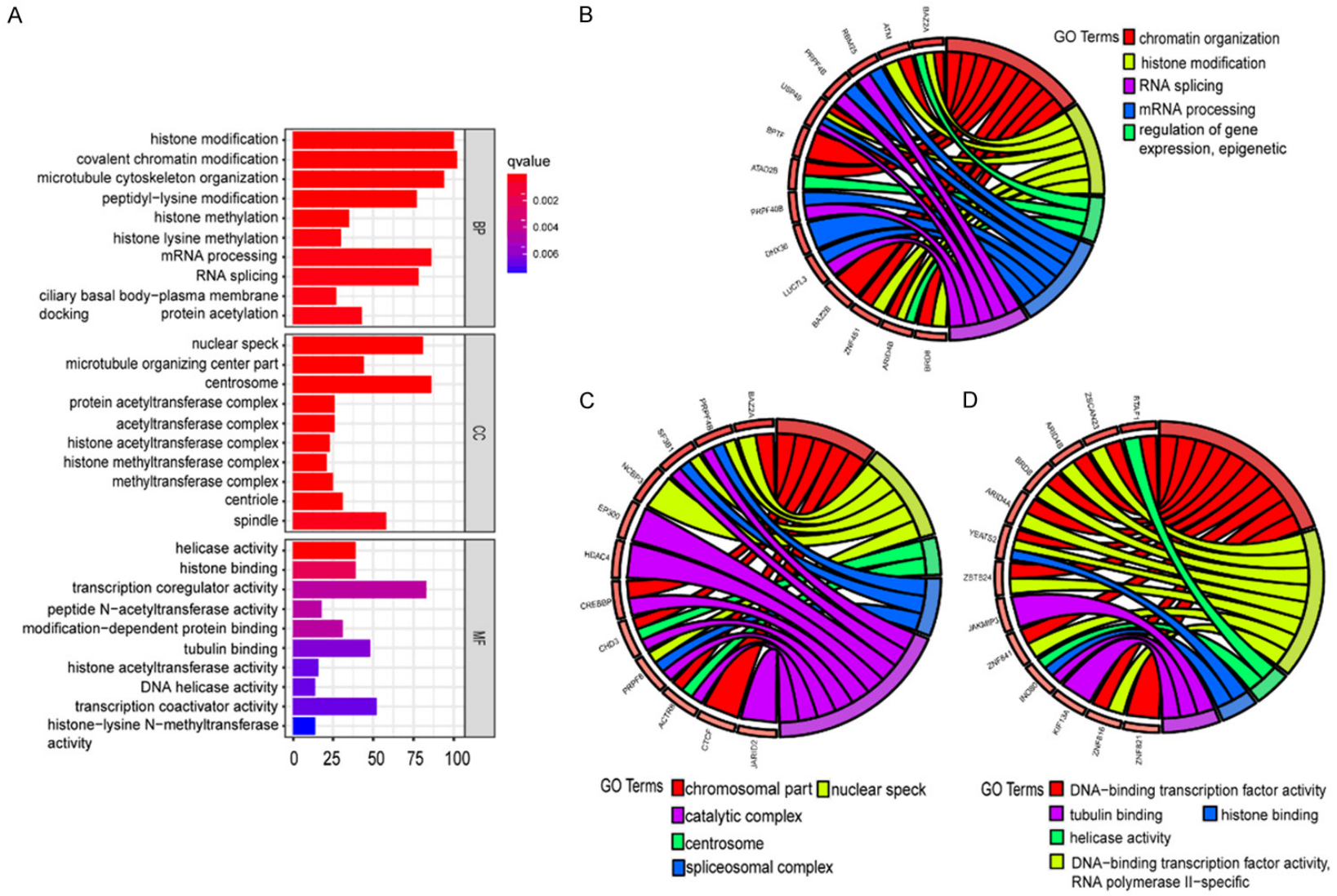
A
histone modification
covalent chromatin modification
microtubule cytoskeleton organization
peptidyl−lysine modification
histone methylation
histone lysine methylation
mRNA processing
RNA splicing
ciliary basal body−plasma membrane docking
protein acetylation
nuclear speck
microtubule organizing center part
centrosome
protein acetyltransferase complex
acetyltransferase complex
histone acetyltransferase complex
histone methyltransferase complex
methyltransferase complex
centriole
spindle
helicase activity
histone binding
transcription coregulator activity
peptide N−acetyltransferase activity
modification−dependent protein binding
tubulin binding
histone acetyltransferase activity
DNA helicase activity
transcription coactivator activity
histone−lysine N−methyltransferase activity
BP
CC
MF
qvalue
0.002
0.004
0.006
0
25
50
75
100
B
GO Terms
chromatin organization
histone modification
RNA splicing
mRNA processing
regulation of gene expression, epigenetic
C
GO Terms
chromosomal part
nuclear speck
catalytic complex
centrosome
spliceosomal complex
D
GO Terms
DNA−binding transcription factor activity
tubulin binding
histone binding
helicase activity
DNA−binding transcription factor activity, RNA polymerase II−specific

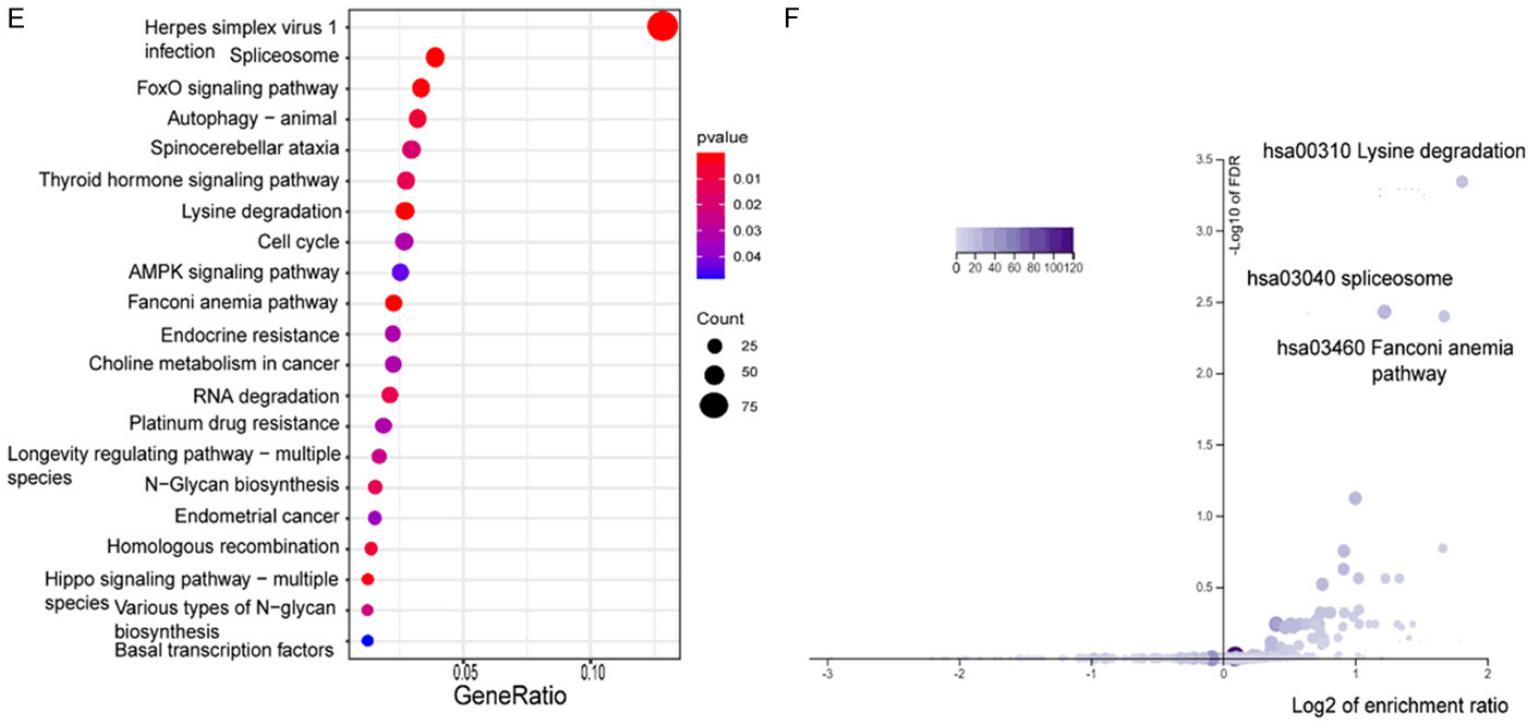

Figure 9. A functional enrichment analysis of the eRNA-target genes. A. Bar plots showing the gene ontology (GO) terms the eRNA-target genes are enriched in. B. Validating the result of the GO-BP (GO-term- Biological Process) analysis in the WEB-based Gene Set Analysis Toolkit. C. Validating the result of the GO-CC (GO-Cellular Component) analysis in the WEB-based Gene Set Analysis Toolkit. D. Validating the result of the GO-MF (GO term-Molecular Function) analysis in the WEB-based Gene Set Analysis Toolkit. E. A bubble plot showing the results of the *Kyoto Encyclopedia of Genes and Genomes* (KEGG) analyses for the eRNA-target genes. F. The KEGG analysis in the WEB-based Gene Set Analysis Toolkit.

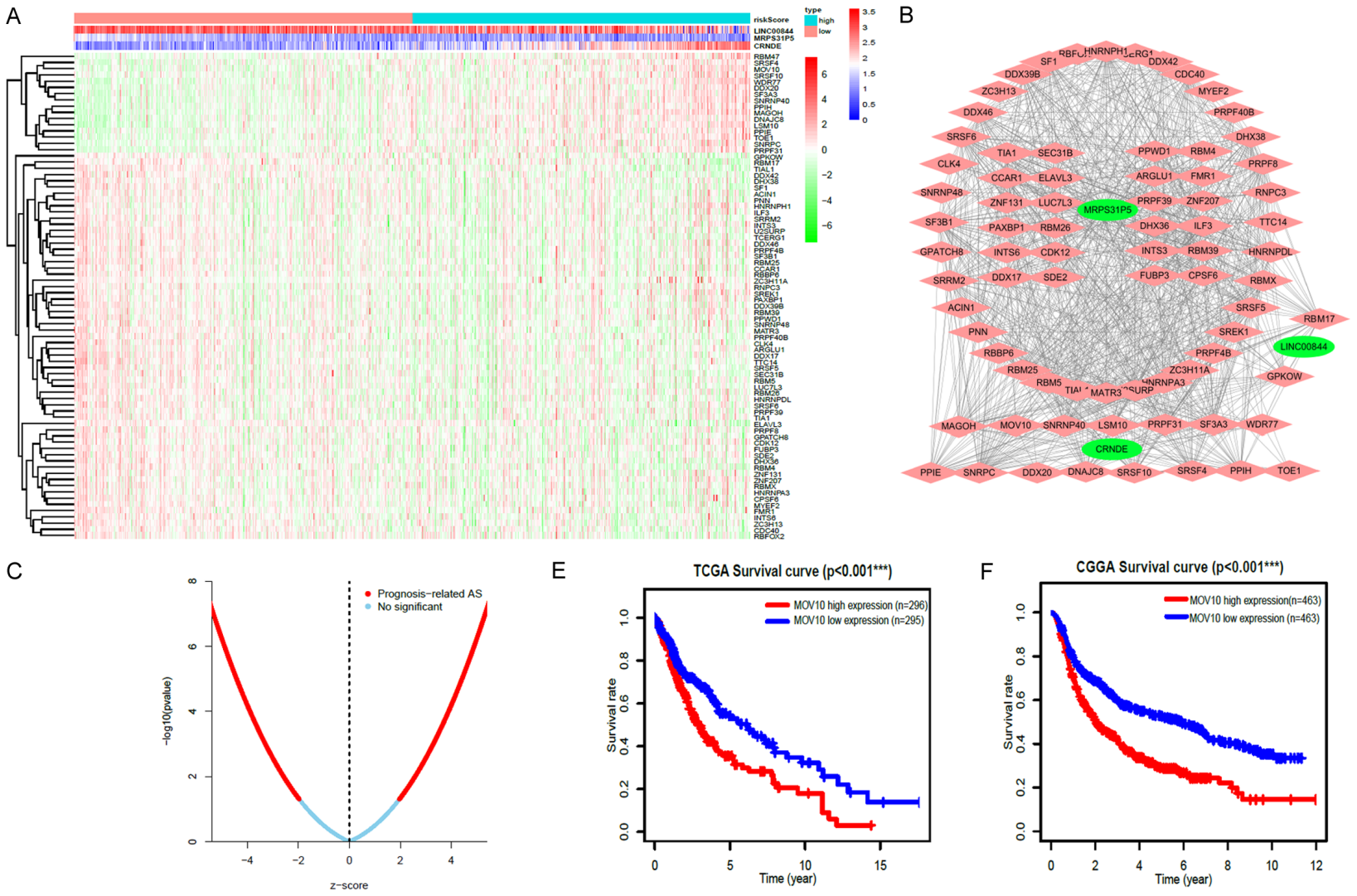
A
riskScore
LINC00844
MRPS31P5
CRNDE
type
high
low
B
MRPS31P5
LINC00844
CRNDE
C
Prognosis−related AS
No significant
−log10(pvalue)
z−score
E
TCGA Survival curve (p<0.001***)
MOV10 high expression (n=296)
MOV10 low expression (n=295)
Survival rate
Time (year)
F
CGGA Survival curve (p<0.001***)
MOV10 high expression(n=463)
MOV10 low expression (n=463)
Survival rate
Time (year)

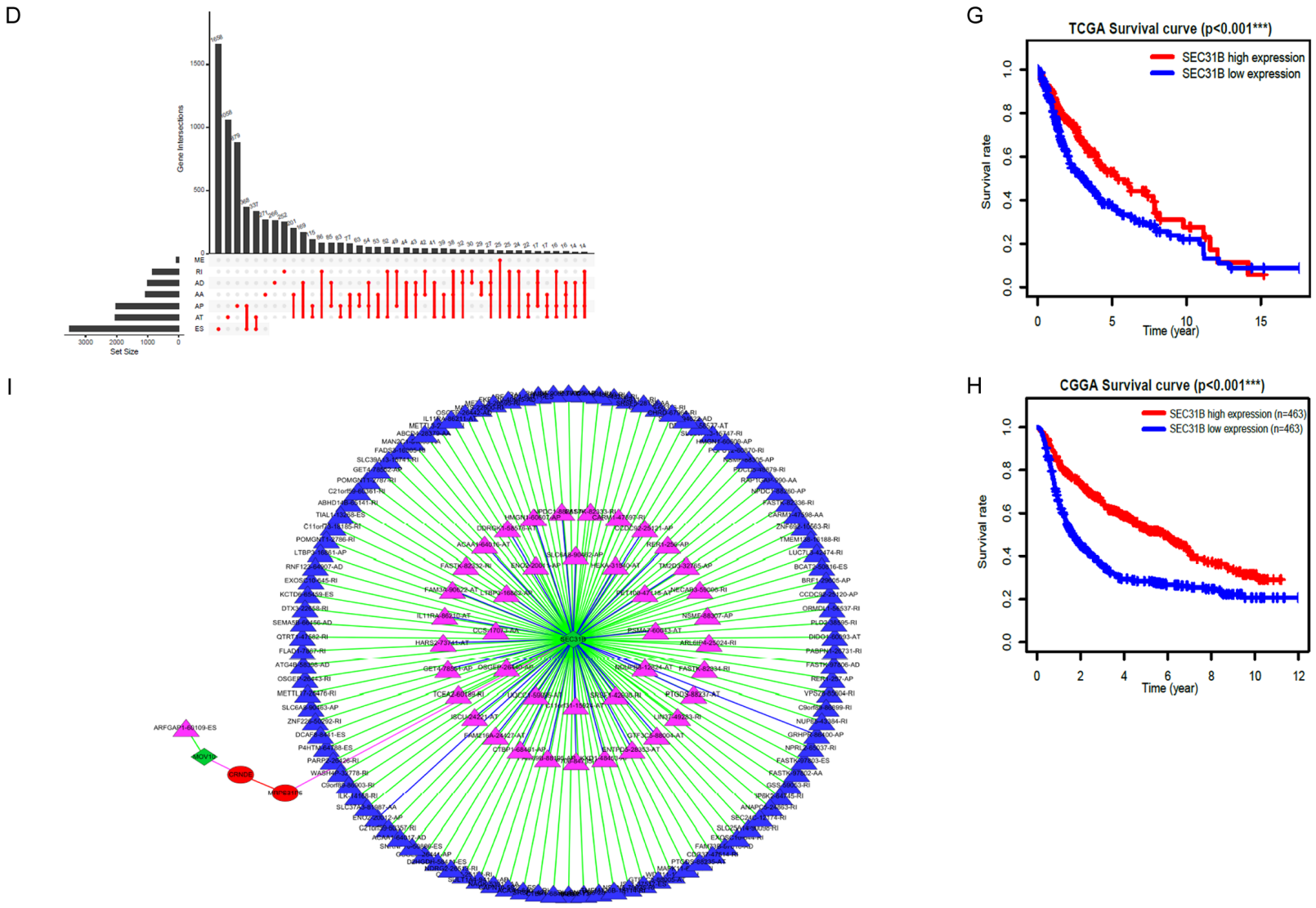

Figure 10. eRNAs and the alternative splicing events. A. A heatmap showing the association between the expressions of the splicing factors and the hub eRNA. B. A network showing the correlation between the hub eRNAs and their targeted splicing factors. C. A volcano map showing the relationships between the alternative events and the glioma prognoses. D. An upset map showing the prognosis-related alternative events. E. A Kaplan-Meier survival curve showing the effect of the MOV10 expression on the overall survival of the glioma patients in the TCGA cohort. F. A Kaplan-Meier survival curve depicting the effect of the MOV10 expressions

on the overall survival of the glioma patients in the CGGA cohort. G. A Kaplan-Meier survival curve showing the effect of SEC31B expression on the overall survival of the glioma patients in the TCGA cohort. H. A Kaplan-Meier survival curve showing the effect of the SEC31B expressions on the overall survival of the glioma patients in the CGGA cohort. I. The network of eRNA-key splicing factor-prognosis-associated AS events. Red circles: hub eRNAs; green diamond: key splicing factors; purple triangle: positive regulation AS events; blue triangle: negative regulation AS events. MOV10: Mov10 RISC Complex RNA Helicase; SEC31B: secretory pathway component Sec31 homolog B, COPII Coat Complex Component. *, $P<0.05$; **, $P<0.01$; ***, $P<0.001$.

validated using the CGGA and Rembrandt cohorts. The risk signature was associated with the clinicopathological features of glioma, including age, grade, the 1p19q codel status, and the IDH status. In addition, we established eRNA-target gene regulatory networks. Our functional analysis revealed that the risk signature is associated with histone modification, histone binding, and RNA processing, which are critical for glioma proliferation. In a nutshell, the risk signature may be utilized as a prognostic biomarker for glioma. However, the correlation between the transcripts does not necessarily infer a causal relationship. Meanwhile, whether these genes are functional components of enhancer activities should be further explored.

Acknowledgements

We would like to thank Mr. Zongtai Zheng, Mr. Zesen Chen, and Mr. Edison Zhang for the data processing and the people who contribute to public biomedical databases. This research was financially supported by the National Natural Science Foundation of China (No. 81901250), the High-Level Hospital Construction Project of Guangdong Province, China (No. DFJH201924), and the Natural Science Foundation of Guangdong Province, China (No. 2018A0303130236). This study was approved by the Research Ethics Committee of Guangdong Provincial People's Hospital, Guangdong Academy of Medical Science (No. GDREC20190145H(R2)). All the patients provided a written informed consent.

Disclosure of conflict of interest

None.

Address correspondence to: Drs. Peng Wang and Dong Zhou, Department of Neurosurgery, Guangdong Provincial People's Hospital, Guangdong Academy of Medical Sciences, No. 106, Zhongshan Second Road, Guangzhou 510080, Guangdong Province, P. R. China. Tel: +86-20-83827812-61521; Fax: +86-20-83827812-61521; E-mail: wangpeng_82@sina.com (PW); zhoudong5413@163.com (DZ)

References

[1] Louis DN, Perry A, Reifenberger G, von Deimling A, Figarella-Branger D, Cavenee WK, Ohgaki H, Wiestler OD, Kleihues P and Ellison DW. The 2016 World Health Organization Classification of tumors of the central nervous system: a summary. Acta Neuropathol 2016; 131: 803-820.

[2] Omuro A and DeAngelis LM. Glioblastoma and other malignant gliomas: a clinical review. JAMA 2013; 310: 1842-1850.

[3] Li W, Notani D and Rosenfeld MG. Enhancers as non-coding RNA transcription units: recent insights and future perspectives. Nat Rev Genet 2016; 17: 207-223.

[4] Bal E, Park HS, Belaid-Choucair Z, Kayserili H, Naville M, Madrange M, Chiticariu E, Hadj-Rabia S, Cagnard N, Kuonen F, Bachmann D, Huber M, Le Gall C, Côté F, Hanein S, Rosti R, Aslanger AD, Waisfisz Q, Bodemer C, Hermine O, Morice-Picard F, Labeille B, Caux F, Mazereeuw-Hautier J, Philip N, Levy N, Taieb A, Avril MF, Headon DJ, Gyapay G, Magnaldo T, Fraitag S, Crollius HR, Vabres P, Hohl D, Munnich A and Smahi A. Mutations in ACTRT1 and its enhancer RNA elements lead to aberrant activation of Hedgehog signaling in inherited and sporadic basal cell carcinomas. Nat Med 2017; 23: 1226-1233.

[5] Gu X, Wang L, Boldrup L, Coates PJ, Fahraeus R, Sgaramella N, Wilms T and Nylander K. AP001056.1, a prognosis-related enhancer RNA in squamous cell carcinoma of the head and neck. Cancers (Basel) 2019; 11: 347.

[6] Chen H, Li C, Peng X, Zhou Z, Weinstein JN; Cancer Genome Atlas Research Network, Liang H. A pan-cancer analysis of enhancer expression in nearly 9000 patient samples. Cell 2018; 173: 386-399, e312.

[7] Vučićević D, Corradin O, Ntini E, Scacheri PC and Ørom UA. Long ncRNA expression associates with tissue-specific enhancers. Cell Cycle 2015; 14: 253-260.

[8] Hoo ZH, Candlish J and Teare D. What is an ROC curve? Emerg Med J 2017; 34: 357-359.

[9] Peng Z, Liu C and Wu M. New insights into long noncoding RNAs and their roles in glioma. Mol Cancer 2018; 17: 61.
[10] Natoli G and Andrau JC. Noncoding transcription at enhancers: general principles and functional models. Annu Rev Genet 2012; 46: 1-19.
[11] Carullo NVN, Phillips Iii RA, Simon RC, Soto SAR, Hinds JE, Salisbury AJ, Revanna JS, Bunner KD, Ianov L, Sultan FA, Savell KE, Gersbach CA and Day JJ. Enhancer RNAs predict enhancer-gene regulatory links and are critical for enhancer function in neuronal systems. Nucleic Acids Res 2020; 48: 9550-9570.
[12] Schaukowitch K, Joo JY, Liu X, Watts JK, Martinez C and Kim TK. Enhancer RNA facilitates NELF release from immediate early genes. Mol Cell 2014; 56: 29-42.
[13] Kim TK, Hemberg M, Gray JM, Costa AM, Bear DM, Wu J, Harmin DA, Laptewicz M, Barbara-Haley K, Kuersten S, Markenscoff-Papadimitriou E, Kuhl D, Bito H, Worley PF, Kreiman G and Greenberg ME. Widespread transcription at neuronal activity-regulated enhancers. Nature 2010; 465: 182-187.
[14] Bhattarai S, Akella A, Gandhi A and Dharap A. Modulation of brain pathology by enhancer RNAs in cerebral ischemia. Mol Neurobiol 2021; 58: 1482-1490.
[15] Zhu Q, Wu Y, Yang M, Wang Z, Zhang H, Jiang X, Chen M, Jin T and Wang T. IRX5 promotes colorectal cancer metastasis by negatively regulating the core components of the RHOA pathway. Mol Carcinog 2019; 58: 2065-2076.
[16] Huang L, Song F, Sun H, Zhang L and Huang C. IRX5 promotes NF-κB signalling to increase proliferation, migration and invasion via OPN in tongue squamous cell carcinoma. J Cell Mol Med 2018; 22: 3899-3910.
[17] Liu T, Zhang X, Yang YM, Du LT and Wang CX. Increased expression of the long noncoding RNA CRNDE-h indicates a poor prognosis in colorectal cancer, and is positively correlated with IRX5 mRNA expression. Onco Targets Ther 2016; 9: 1437-1448.
[18] Zhou W, Huang K, Zhang Q, Ye S, Zhong Z, Zeng C, Peng G, Li L and Ye Q. LINC00844 promotes proliferation and migration of hepatocellular carcinoma by regulating NDRG1 expression. PeerJ 2020; 8: e8394.
[19] Qiu K, Zheng Z and Huang Y. Long intergenic noncoding RNA 00844 promotes apoptosis and represses proliferation of prostate cancer cells through upregulating GSTP1 by recruiting EBF1. J Cell Physiol 2020; 235: 8472-8485.
[20] Lingadahalli S, Jadhao S, Sung YY, Chen M, Hu L, Chen X and Cheung E. Novel lncRNA LINC00844 regulates prostate cancer cell migration and invasion through AR signaling. Mol Cancer Res 2018; 16: 1865-1878.
[21] Fu H, Ge B, Chen D, Wu Y, Luo Q, Li X, Zheng C and Tang Q. Phytanoyl-CoA 2-hydroxylase-interacting protein-like gene is a therapeutic target gene for glioblastoma multiforme. Med Sci Monit 2019; 25: 2583-2590.
[22] Leonhardt K, Gebhardt R, Mössner J, Lutsenko S and Huster D. Functional interactions of Cu-ATPase ATP7B with cisplatin and the role of ATP7B in the resistance of cells to the drug. J Biol Chem 2009; 284: 7793-7802.
[23] Petruzzelli R and Polishchuk RS. Activity and trafficking of copper-transporting ATPases in tumor development and defense against platinum-based drugs. Cells 2019; 8: 1080.
[24] Miller SL, Antico G, Raghunath PN, Tomaszewski JE and Clevenger CV. Nek3 kinase regulates prolactin-mediated cytoskeletal reorganization and motility of breast cancer cells. Oncogene 2007; 26: 4668-4678.
[25] Ransohoff JD, Wei Y and Khavari PA. The functions and unique features of long intergenic non-coding RNA. Nat Rev Mol Cell Biol 2018; 19: 143-157.
[26] Chen H, Du G, Song X and Li L. Non-coding transcripts from enhancers: new insights into enhancer activity and gene expression regulation. Genomics Proteomics Bioinformatics 2017; 15: 201-207.
[27] Ellis BC, Molloy PL and Graham LD. CRNDE: a long non-coding RNA involved in CanceR, neurobiology, and development. Front Genet 2012; 3: 270.
[28] Zhang J, Yin M, Peng G and Zhao Y. CRNDE: an important oncogenic long non-coding RNA in human cancers. Cell Prolif 2018; 51: e12440-e12440.
[29] Lee Y and Rio DC. Mechanisms and regulation of alternative pre-mRNA splicing. Annu Rev Biochem 2015; 84: 291-323.
[30] Lee SC and Abdel-Wahab O. Therapeutic targeting of splicing in cancer. Nat Med 2016; 22: 976-986.
[31] Anczukow O and Krainer AR. Splicing-factor alterations in cancers. RNA 2016; 22: 1285-1301.
[32] Nakano M, Kakiuchi Y, Shimada Y, Ohyama M, Ogiwara Y, Sasaki-Higashiyama N, Yano N, Ikeda F, Yamada E, Iwamatsu A, Kobayashi K, Nishiyama K, Ichikawa S, Kaji K, Ide T, Murofushi H and Murakami-Murofushi K. MOV10 as a novel telomerase-associated protein. Biochem Biophys Res Commun 2009; 388: 328-332.
[33] Skariah G, Seimetz J, Norsworthy M, Lannom MC, Kenny PJ, Elrakhawy M, Forsthoefel C, Drnevich J, Kalsotra A and Ceman S. Mov10 suppresses retroelements and regulates neuronal

development and function in the developing brain. BMC Biol 2017; 15: 54.
[34] Skariah G, Perry KJ, Drnevich J, Henry JJ and Ceman S. RNA helicase Mov10 is essential for gastrulation and central nervous system development. Dev Dyn 2018; 247: 660-671.
[35] Kenny PJ, Zhou H, Kim M, Skariah G, Khetani RS, Drnevich J, Arcila ML, Kosik KS and Ceman S. MOV10 and FMRP regulate AGO2 association with microRNA recognition elements. Cell Rep 2014; 9: 1729-1741.
[36] He Q, Zhao L, Liu X, Zheng J, Liu Y, Liu L, Ma J, Cai H, Li Z and Xue Y. MOV10 binding circ-DICER1 regulates the angiogenesis of glioma via miR-103a-3p/miR-382-5p mediated ZIC4 expression change. J Exp Clin Cancer Res 2019; 38: 9.
[37] Stankewich MC, Stabach PR and Morrow JS. Human Sec31B: a family of new mammalian orthologues of yeast Sec31p that associate with the COPII coat. J Cell Sci 2006; 119: 958-969.
[38] Niu X, Hong J, Zheng X, Melville DB, Knapik EW, Meng A and Peng J. The nuclear pore complex function of Sec13 protein is required for cell survival during retinal development. J Biol Chem 2014; 289: 11971-11985.

Supplementary Table 1. The clinicopathological characteristics in patients with glioma from Guangdong Provincial People's Hospital

Parameters	Number	Percentage (%)
Age		
<60 years	29	72.5
≥60 years	11	17.5
Gender		
Male	24	60
Female	16	40
Location		
Frontal Lobe	16	40
Occipital Lobe	2	5
Parietal Lobe	5	12.5
Temporal Lobe	10	25
Brain Stem	5	12.5
Cerebellum	2	5
Grade		
II	11	27.5
III	12	30
IV	17	42.5
Isocitrate dehydrogenase status		
Wild Type	20	50
Mutant	19	47.5
NA	1	2.5
Type		
Astrocytoglioma	10	25
Oligodendroglia glioma	3	7.5
Anaplastic astrocytoglioma	4	10
Anaplastic oligodendroglia glioma	5	12.5
Glioblastoma	18	45

Supplementary Table 2. Hub eRNAs and its targeted SFs

eRNA	Correlation	*P*-value	Targeted SFs
CRNDE	0.47	0	SF3A3
	0.415	0	SNRPC
	0.463	0	PPIH
	0.424	0	PRPF31
	0.534	0	WDR77
	0.445	0	DNAJC8
	0.516	0	MAGOH
	0.401	0	DDX20
	0.481	0	LSM10
	0.404	8.35E-29	SRSF4
	0.437	0	MOV10
	0.453	1.56E-36	SRSF10
	0.425	0	PPIE
	0.504	0	SNRNP40
	0.431	0	TOE1
MRPS31P5	0.475	1.23E-40	CLK4
	0.618	8.22E-75	U2SURP
	0.452	2.15E-36	ZNF131
	0.51	1.88E-47	INTS6
	0.415	1.66E-30	TIAL1
	0.507	5.98E-47	SRSF6
	0.466	5.61E-39	CCAR1
	0.487	6.08E-43	RBBP6
	0.465	1.19E-38	PRPF39
	0.598	5.42E-69	RBM26
	0.621	9.42E-76	GPATCH8
	0.469	2.04E-39	SNRNP48
	0.536	3.64E-53	RNPC3
	0.559	1.53E-58	ARGLU1
	0.441	1.68E-34	CDC40
	0.433	2.63E-33	HNRNPH1
	0.458	1.61E-37	FMR1
	0.477	7.22E-41	DHX38
	0.595	4.74E-68	CPSF6
	0.411	8.56E-30	PRPF8
	0.635	5.46E-80	TCERG1
	0.504	2.87E-46	RBM5
	0.434	2.03E-33	RBFOX2
	0.555	1.47E-57	LUC7L3
	0.648	2.05E-84	DDX17
	0.519	2.27E-49	PAXBP1
	0.414	2.95E-30	SDE2
	0.637	8.15E-81	TTC14
	0.472	4.22E-40	RBM39
	0.596	2.43E-68	DDX39B
	0.456	4.30E-37	ZNF207

	0.557	3.15E-58	PRPF40B
	0.589	1.82E-66	RBM25
	0.56	8.28E-59	SRRM2
	0.616	4.08E-74	MATR3
	0.496	1.31E-44	TIA1
	0.441	1.18E-34	FUBP3
	0.476	1.13E-40	CDK12
	0.427	2.41E-32	RBM4
	0.486	1.32E-42	SEC31B
	0.575	1.28E-62	MYEF2
	0.584	5.82E-65	PRPF4B
	0.438	3.92E-34	DDX42
	0.536	4.45E-53	DDX46
	0.415	2.05E-30	ILF3
	0.527	4.51E-51	INTS3
	0.487	8.54E-43	SF1
	0.512	6.45E-48	ZC3H13
	0.481	1.28E-41	HNRNPDL
	0.58	5.44E-64	SF3B1
	0.442	9.57E-35	ACIN1
	0.552	6.73E-57	ZC3H11A
	0.447	1.49E-35	RBMX
	0.483	4.25E-42	HNRNPA3
	0.483	4.46E-42	SREK1
	0.49	1.64E-43	SRSF5
	0.522	3.95E-50	PNN
	0.555	1.02E-57	DHX36
	0.519	2.61E-49	PPWD1
	0.412	5.44E-30	ELAVL3
LINC00844	0.453	1.31E-36	RBM17
	0.452	1.94E-36	GPKOW

SF: splicing factor. SFs with correlation coef >0.4, *P*-value <0.05 were regarded as targeted SFs.